

## Supporting Information for

### Expanding the scope of antibody rebridging with new pyridazinedione-TCO constructs

Angela N. Marquard<sup>#1</sup>, Jonathan C. T. Carlson<sup>+1,2</sup>, Ralph Weissleder<sup>1,3</sup>

<sup>1</sup>Center for Systems Biology, Massachusetts General Hospital Research Institute, Boston, MA 02114

<sup>2</sup>Cancer Center, Massachusetts General Hospital and Harvard Medical School, Boston, MA 02114

<sup>3</sup>Department of Systems Biology, Harvard Medical School, Boston, MA 02115

+ Jonathan CT Carlson, MD, PhD  
Center for Systems Biology  
Massachusetts General Hospital  
185 Cambridge St, CPZN 5206  
Boston, MA, 02114  
carlson.jonathan@mgh.harvard.edu

#### Table of Contents

|  |         |
|--|---------|
| Figure S1. Cellular staining with rebridged TCO-rituximab        | S2      |
| Figure S2. SDS-PAGE of barcoded cetuximab                        | S3      |
| Figure S3. SDS-PAGE of rebridged antibodies                      | S4      |
| Table S1. Antibodies tested                                      | S5      |
| Figure S4. Labeling of individual antibodies                     | S5      |
| Figure S5. Cellular staining with rebridged mouse IgG2a antibody | S6      |
| Figure S6. Cellular staining with rebridged rat IgG2b antibody   | S7      |
| Figure S7 and S8. Characterization of mouse IgG1 antibody        | S8-S9   |
| Figure S9. Antibody subclass structures                          | S10     |
| Cellular staining conditions                                     | S11     |
| Cetuximab-barcode preparation                                    | S12     |
| Synthesis  | S13-S14 |
| NMR Spectra  | S15-S18 |
| References   | S19     |

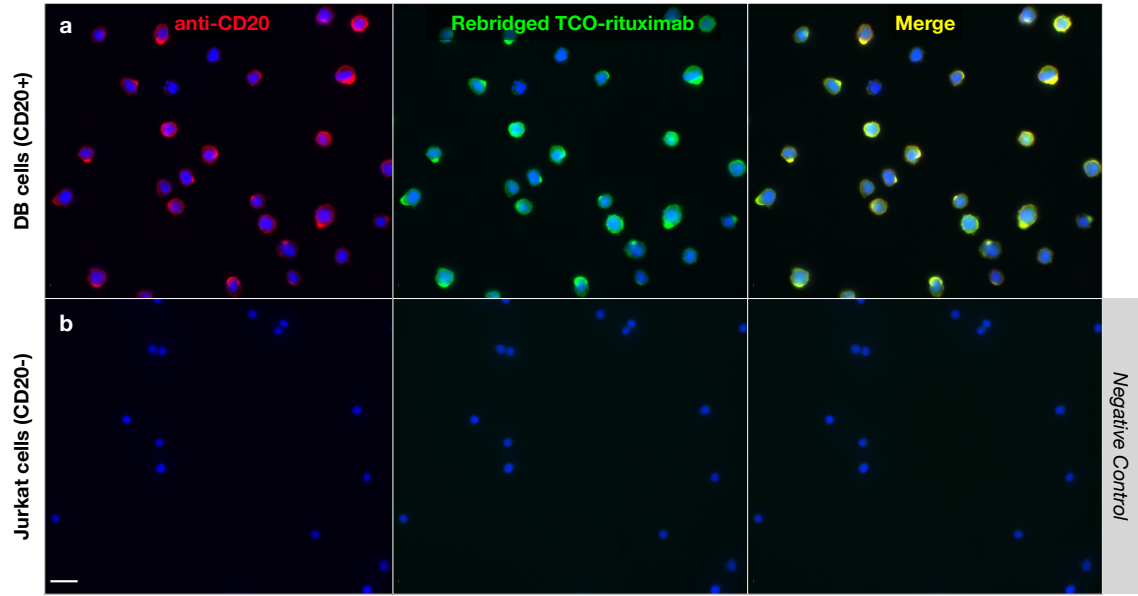


**Figure S1.** Cellular staining with rebridged TCO-rituximab. a) CD20+ DB cells were co-stained with a control anti-CD20 antibody (red) and rebridged TCO-rituximab (green), as well as DAPI for nuclear reference. Merged images demonstrate good colocalization. b) CD20- Jurkat cells stained in parallel; no non-specific staining is observed. Scale bar = 20  $\mu\text{m}$ .

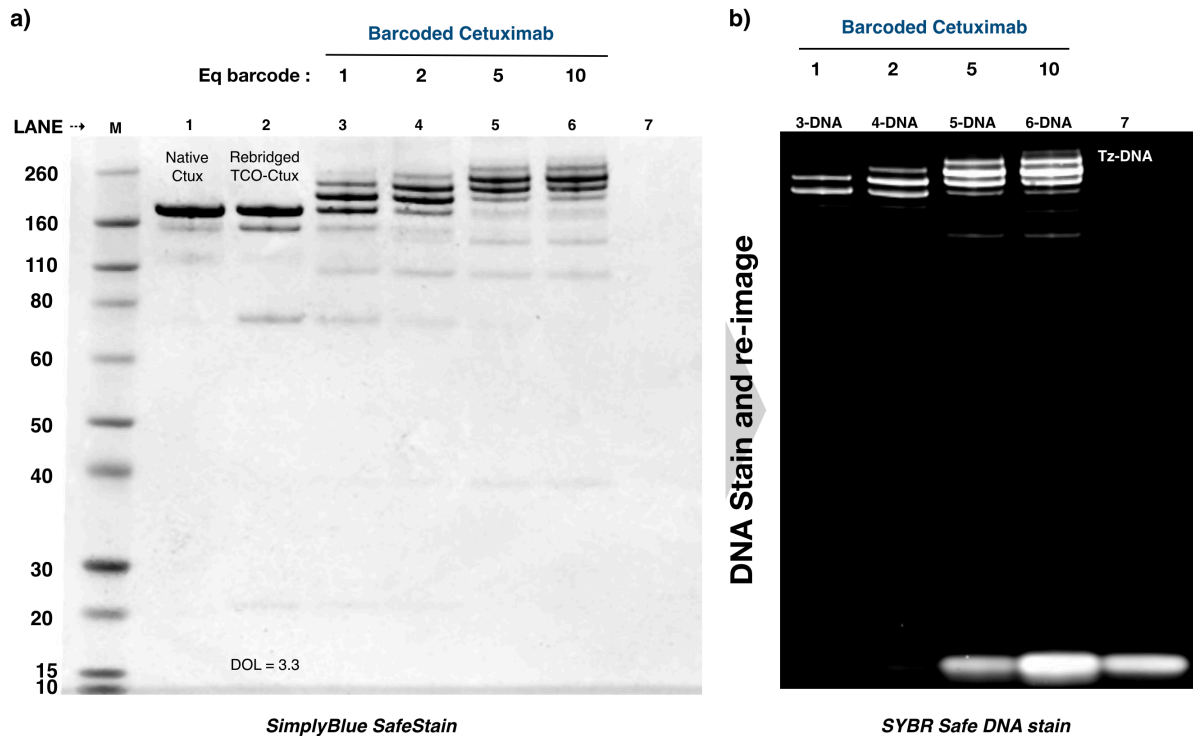


**Figure S2.** Cetuximab was rebridged with PD-TCO **1** (DOL = 3.3) then treated with increasing equivalents of a Tz-DNA barcode with no purification. a) SDS-PAGE of rebridged and barcoded cetuximab. M: protein molecular weight marker in kDa; 1: native cetuximab; 2: TCO-cetuximab rebridged with **1** (DOL = 3.3); 3-6: TCO-cetuximab treated with 1, 2, 5, and 10 equivalents Tz-DNA barcode, respectively. A distribution of bands corresponding to 0-4 barcodes/antibody is present. Gel stained with SimplyBlue SafeStain. b) Barcoded cetuximab in lanes 3-6 of the same gel remained with SYBR Safe DNA gel stain and re-imaged. A distribution of bands corresponding to 1-4 barcodes/antibody are present; Lane 7: Tz-DNA only. When a substoichiometric amount of DNA is used, no detectable free DNA is present (Lanes 3-DNA and 4-DNA) eliminating the need for purification.

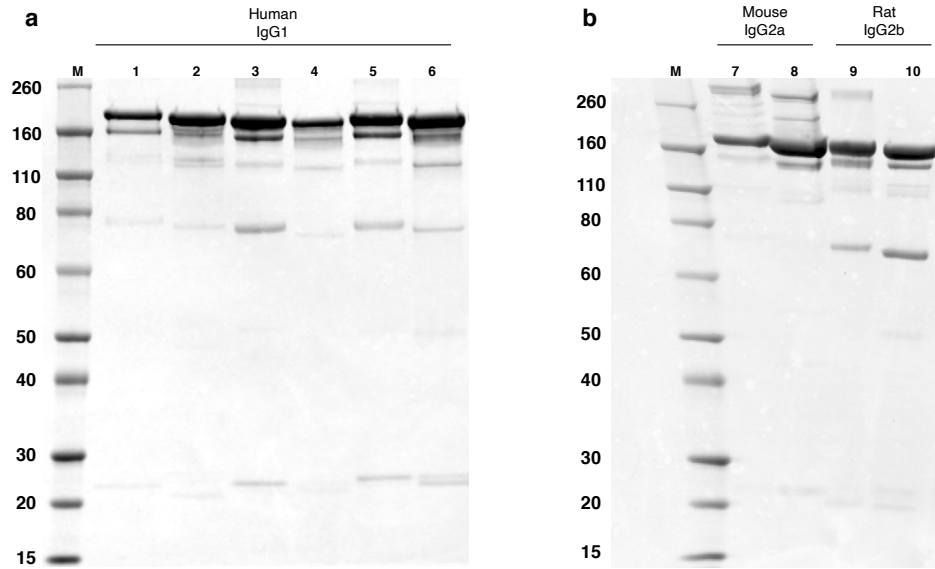


**Figure S3.** a) SDS-PAGE of human IgG1 antibodies: M: molecular weight marker in kDa; 1: rebridged cetuximab (DOL = 3.2); 2: native cetuximab; 3: rebridged rituximab (DOL = 3.1); 4: native rituximab; 5: rebridged trastuzumab (DOL = 3.9); 6: native trastuzumab. b) SDS-PAGE of mouse and rat IgG antibodies: M: molecular weight marker in kDa; 7: rebridged mouse IgG2a antibody (anti-hu CD8a, DOL = 4.0); 8: native mouse IgG2a antibody (anti-hu CD8a); 9: rebridged rat IgG2b antibody (anti-ms CD3, DOL = 4.5); 10: native rat IgG2b antibody (anti-ms CD3).

| Host Species   | Isotype | Antibody               | Clone      | Vendor                    | Cat. No. | # Disulfides | PD DOL        | Labeling % |
|----------------|---------|------------------------|------------|---------------------------|----------|--------------|---------------|------------|
| Human          | IgG1    | Trastuzumab (lit)      |            |                           |          | 4            | 4.0           | 100        |
|                |         | Trastuzumab            |            |                           |          | 4            | 3.7 ± 0.4     | 93         |
|                |         | Cetuximab              |            |                           |          | 4            | 3.2 ± 0.2     | 80         |
|                |         | Rituximab              |            |                           |          | 4            | 3.2 ± 0.3     | 80         |
|                | IgG4    | Pembrolizumab          | 29F.1A12   |                           |          | 4            | 1.3 ± 0.4     | 31         |
| Mouse          | IgG1    | anti-human CD3         | UCHT1      | Bioxcell                  | BE0231   | 5            | 1.3 ± 0.2     | 25         |
|                |         | anti-human CD45        | 2D1        | BioLegend                 | 368502   | 5            | 1.1 ± 0.6     | 23         |
|                | IgG2a   | anti-human CD8a        | OKT-8      | Bioxcell                  | BE0004-2 | 5            | 3.8 ± 0.3     | 76         |
|                |         | anti-human PD-L1       | ABM4E54    | abcam                     | 210931   | 5            | 3.1 ± 0.3     | 63         |
|                |         | anti-human CD3         | OKT3       | BioLegend                 | 317302   | 5            | 3.7 ± 0.1     | 73         |
|                | IgG2b   | anti-human CD20        | 2H7        | BioLegend                 | 302302   | 6            | 2.1 ± 0.2     | 35         |
| anti-human CD4 |         | OKT-4                  | Bioxcell   | BE0003-2                  | 6        | 2.6 ± 0.2    | 43            |            |
| Rat            | IgG1    | anti-mouse CD1d        | 20H2       | Bioxcell                  | BE0179   | 5            | 2.1 ± 0.2     | 42         |
|                |         | anti-mouse CD8a        | 53-6.7     | Bioxcell                  | BE0004-1 | 4            | 1.17 ± 0.05   | 29         |
|                | IgG2a   | anti-mouse CD86        | GL-1       | Bioxcell                  | BE0025   | 4            | 1.1 ± 0.4     | 28         |
|                |         | anti-mouse CD3         | 17A2       | Bioxcell                  | BE0002   | 6            | 4.7 ± 0.2     | 79         |
|                |         | anti-mouse/human CD11b | M1/70      | Bioxcell                  | BE0007   | 6            | 4.5 ± 0.3     | 75         |
|                | IgG2b   | anti-mouse PD-L1       | 10F.9G2    | Bioxcell                  | BE0101   | 6            | 5.0 ± 0.3     | 83         |
|                |         | anti-human CD4         | A161A1     | BioLegend                 | 317402   | 6            | 5.5 ± 0.2     | 92         |
| Rabbit         | IgG     | rabbit IgG isotype     | polyclonal | Bio-Rad                   | PRABP01  | 3            | 0.753 ± 0.004 | 25         |
|                |         | anti-human pS6         | D68F8      | Cell Signaling Technology | 5364BF   | 3            | 1.3 ± 0.9     | 43         |

**Table S1.** List of antibodies and degree of PD-labeling after rebridging with 1

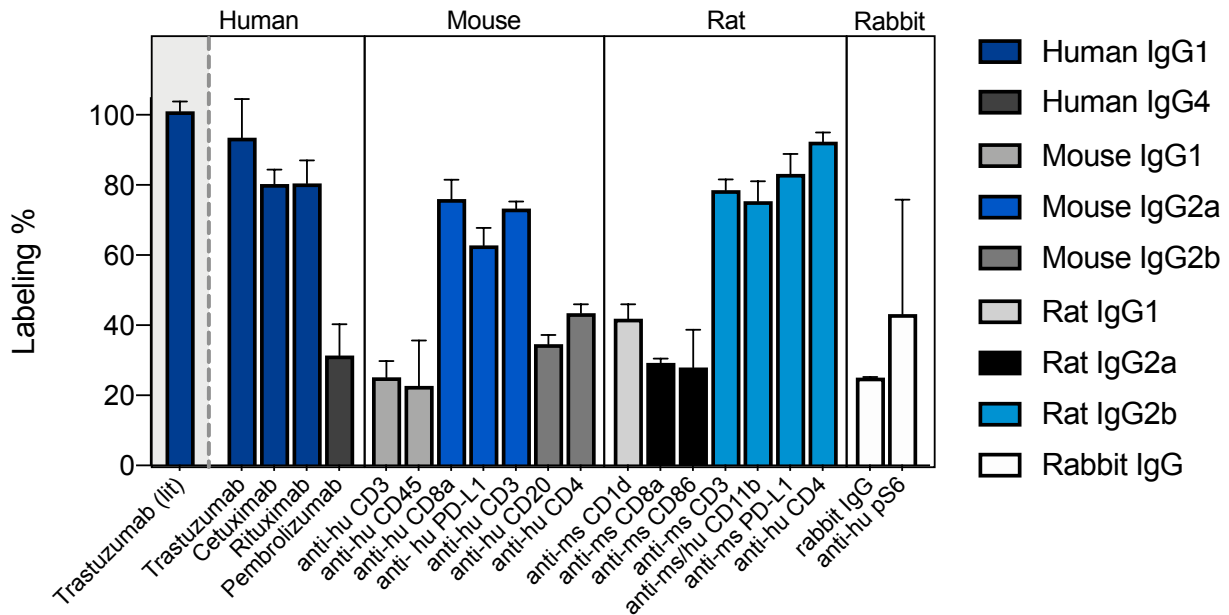


**Figure S4.** PD-labeling of individual antibodies by rebridging with 1

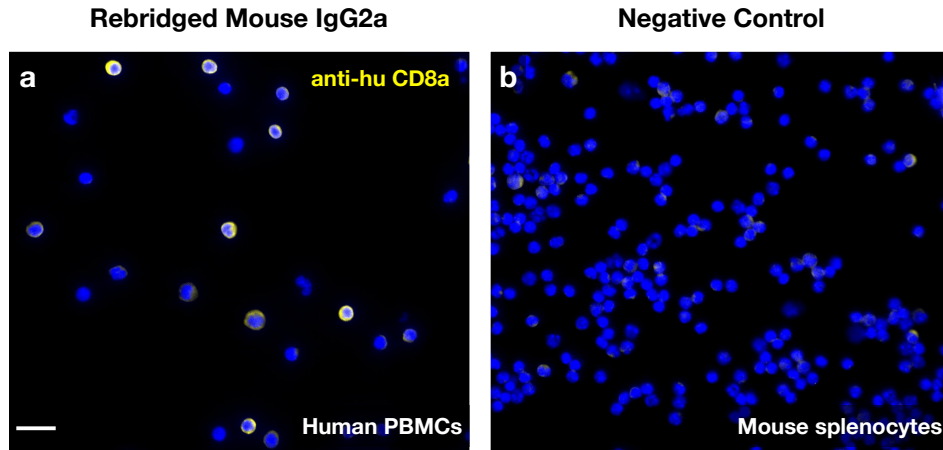


**Figure S5.** Cellular staining with rebridged mouse IgG2a antibody. a) Human peripheral blood mononuclear cells (PBMCs) stained with rebridged anti-human CD8a (mouse IgG2a) T-cell marker. b) Mouse splenocytes stained with rebridged anti-human CD8a as a negative control. Scale bar = 20  $\mu\text{m}$ .

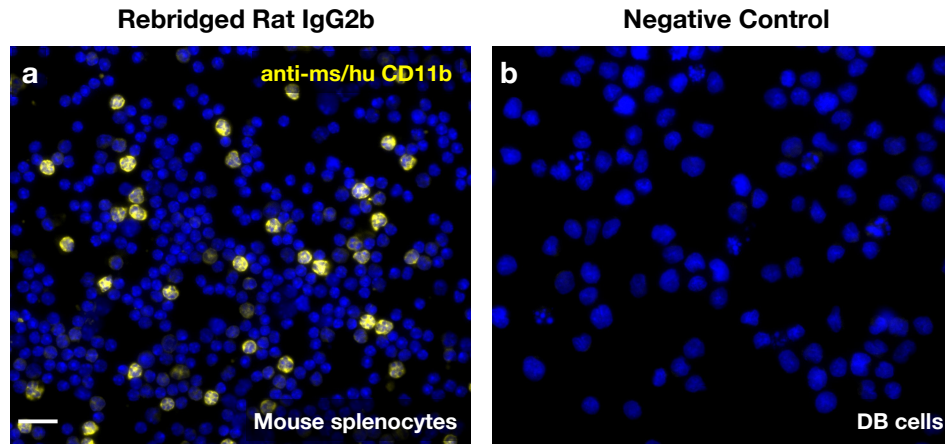


**Figure S6.** Cellular staining with rebridged rat IgG2b antibody. a) Mouse splenocytes stained with rebridged anti-CD11b (rat IgG2b); the antibody for this macrophage marker is both mouse/human reactive. b) CD11b- DB cells (B-cell lymphoma) stained with rebridged anti-mouse/human CD11b as a negative control. Scale bar = 20  $\mu$ m.

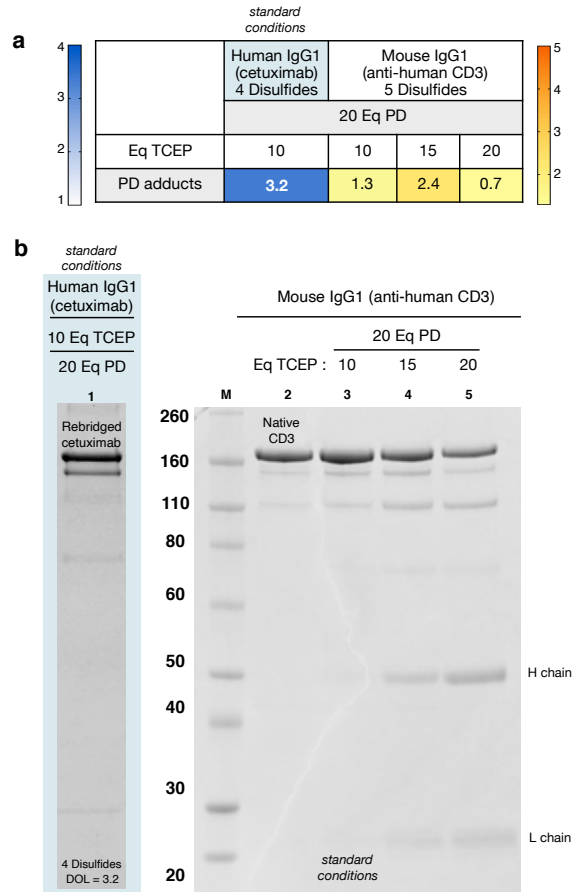


**Figure S7.** Increasing the amount of TCEP does not result in successfully rebridged mouse IgG1 antibodies. a) Number of PD adducts determined by UV-VIs analysis after treating a mouse IgG1 antibody with PD-TCO 1 under increasing amounts of TCEP. Higher equivalents of TCEP to facilitate disulfide reduction still yields poor PD labeling. b) SDS-PAGE: M: molecular weight ladder in kDa; 1: rebridged cetuximab under standard conditions (PD DOL = 3.2); 2: native mouse IgG1 anti-CD3; 3: CD3 under standard rebridging conditions (DOL = 1.3, 26%); 4-5: CD3 under rebridging conditions with increasing amounts of TCEP. At higher TCEP concentrations, mouse IgG1 is reduced to its heavy (H) and light (L) chains. Data for successfully rebridged human IgG1 cetuximab under standard conditions is shown for reference (shaded blue).



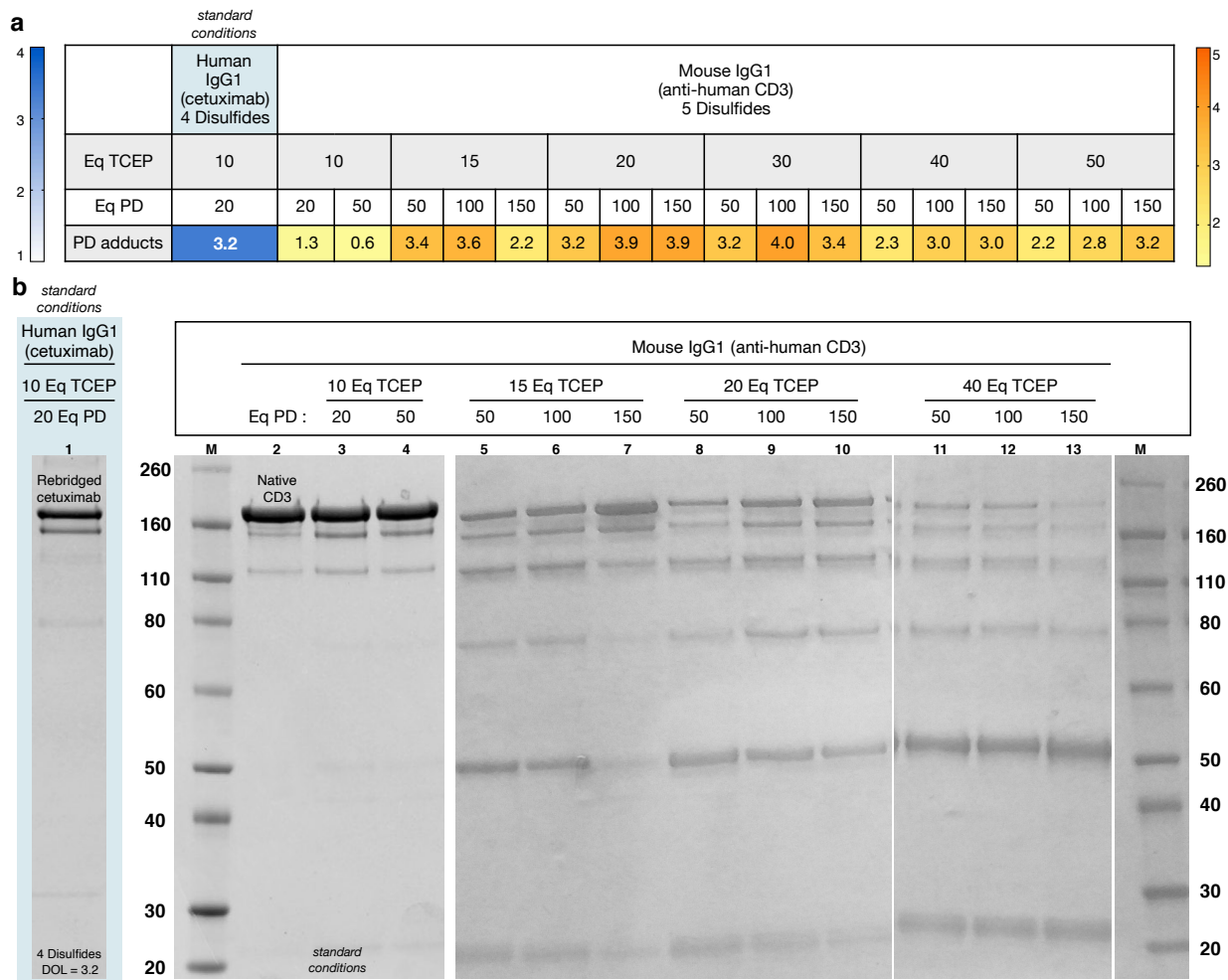


**Figure S8.** A range of conditions with varying amounts of TCEP and PD-TCO 1 were tested and did not yield successfully rebridged mouse IgG1. a) Number of PD adducts determined by UV-Vis analysis after treating a mouse IgG1 antibody with PD-TCO 1 under different reaction conditions. b) SDS-PAGE: M: molecular weight ladder in kDa; 1: rebridged cetuximab under standard conditions (PD DOL = 3.2); 2: native mouse IgG1 anti-CD3; 3: CD3 under standard rebridging conditions (DOL = 1.3, 26%) 4-13: CD3 under rebridging conditions with different amounts of TCEP and PD-TCO 1. All conditions yielded either poor PD labeling (a), mis-rebridged/reduced species (b), or both. Data for successfully rebridged human IgG1 cetuximab under standard conditions is shown for reference (shaded blue).

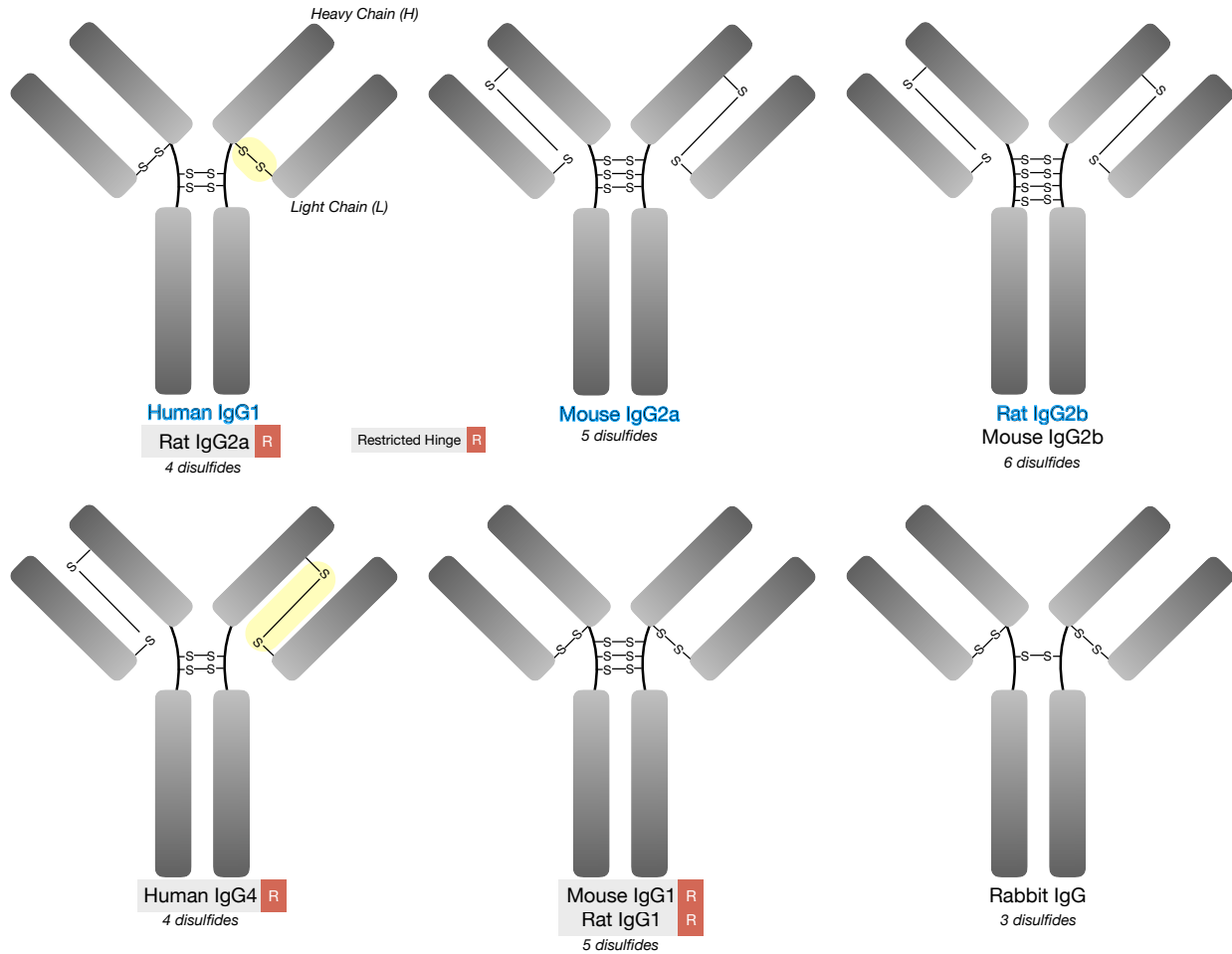


**Figure S9. Comparison of the interchain disulfide structure of isotype subclasses tested.** Antibody subclasses differ in the number of H-H chain disulfides (1-4) and the position of the H-L chain disulfide. The heavy chain cysteine residue involved in the H-L chain connection is either located in the upper hinge region (human IgG1, yellow shading) or nearer the N-terminus in the heavy chain sequence (human IgG4, yellow-shading). Subclasses that have a restricted hinge are denoted by **R**. Isotype subclasses that were rebridged are highlighted in blue. Information in figure compiled from multiple literature sources.<sup>1-4</sup>

## Cellular Staining Conditions

### **TCO-cetuximab in A-431 cells (Figure 2a)**

A-431 cells cultured on a glass slide were fixed with 4% paraformaldehyde and blocked with 2% bovine serum albumin (BSA). Cells were then stained with either 10 µg/mL TCO-cetuximab rebridged with **1** and clicked with a Methyltetrazine-Cy3 fluorophore (Click Chemistry Tools, #1018) or 10 µg/mL unmodified cetuximab followed by staining with Alexa Fluor 488-conjugated anti-human secondary antibody (ThermoFisher). Cells were stained with Hoechst to visualize the nuclei and imaged to compare the cellular staining patterns of rebridged and unmodified cetuximab.

### **TCO-rituximab in DB and Jurkat cells (Figure S1)**

DB (CD20+) and Jurkat (CD20-) cells were fixed with 4% paraformaldehyde and blocked with 2% BSA. Cells were then stained with both 10 µg/mL mouse anti-human CD20 antibody and 10 µg/mL TCO-rituximab rebridged with **1** and clicked with a Tz-AF488 fluorophore (Click Chemistry Tools, #1361) followed by staining with Alexa Fluor 647-conjugated anti-mouse secondary antibody (ThermoFisher). Cells were stained with DAPI and mounted onto a glass slide for imaging.

### **TCO-anti-human CD8a in human PBMCs and mouse splenocytes (Figure S5)**

Human peripheral blood mononuclear cells (PBMCs) were isolated from leukapheresis donors (Massachusetts General Hospital) according to a standard protocol.<sup>5</sup> In brief, whole blood was layered over a column of Ficoll Paque Plus (GE Healthcare) and then centrifuged. The layer of PBMCs was then isolated, washed with HBSS 3 times, fixed with 4% paraformaldehyde, and blocked with 2% BSA. Mouse splenocytes were obtained from single cell homogenate of spleen tissues harvested from C57BL6 mice, fixed with 4% paraformaldehyde and blocked with Odyssey blocking buffer (Li-Cor Biosciences). Cells were deposited onto glass slides using a Thermo Shandon Cytospin 4 centrifuge and the slides were blocked with 2% BSA. Cells were then stained with 10 µg/mL TCO-anti-human CD8a (mouse IgG2a) rebridged with **1** and clicked with a Tz-AF488 fluorophore (Click Chemistry Tools, #1361). Cells were stained with Hoechst to visualize the nuclei and imaged.

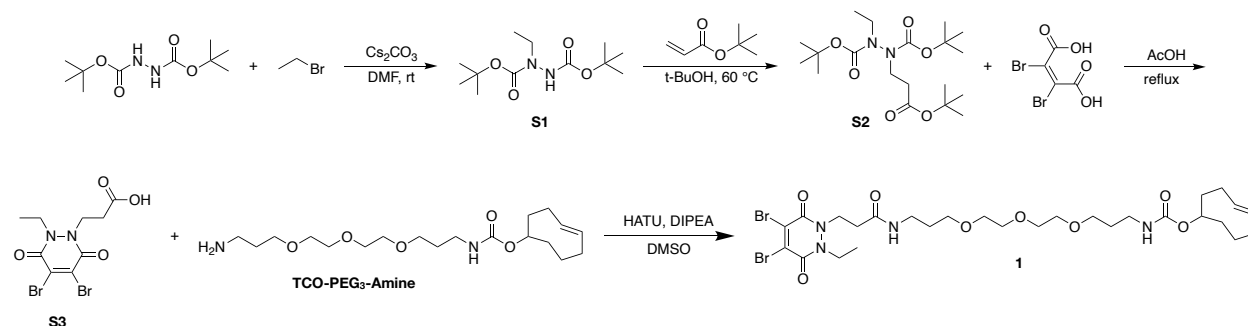
### **TCO-anti-mouse/human CD11b in mouse splenocytes and DB cells (Figure S6)**

Mouse splenocytes were obtained from single cell homogenate of spleen tissues harvested from C57BL6 mice, fixed with 4% paraformaldehyde and blocked with Odyssey blocking buffer (Li-Cor Biosciences). DB cells were fixed with 4% paraformaldehyde and blocked with 2% BSA. Cells were deposited onto glass slides using a Thermo Shandon Cytospin 4 centrifuge and the slides were blocked with 2% BSA. Cells were then stained with 10 µg/mL TCO-anti-mouse/human CD11b (rat IgG2b) rebridged with **1** and clicked with a Tz-AF594 fluorophore (Click Chemistry Tools, #1364). Cells were stained with Hoechst to visualize the nuclei and imaged.

## Cetuximab-Barcode Preparation

Amine-modified DNA barcode (65 nt, Integrated DNA Technologies) was solvent-exchanged with Zeba spin desalting columns (7 K MWCO) into borate buffer (pH 8.5). The DNA was then incubated at room temperature with Methyltetrazine-PEG<sub>4</sub>-NHS (Click Chemistry Tools, #1069, 20 equivalents, 10% DMF in the final reaction mixture). After 25 min, excess NHS ester was removed by three successive Zeba spin desalting columns (7 K MWCO) equilibrated with pH 7 PBS. Tz-DNA was analyzed by UV-Vis spectrometry and Tz:DNA ratio was calculated from absorbance measurements at 520 and 260 nm using the known extinction coefficients of the tetrazine ( $438 \text{ M}^{-1} \text{ cm}^{-1}$ ) and DNA barcode ( $602,500 \text{ M}^{-1} \text{ cm}^{-1}$ , provided by manufacturer). Measurements at two different dilutions were required to account for the much stronger absorbance of the DNA. Cetuximab was modified with PD-TCO **1** as above to yield rebridged TCO-cetuximab (DOL = 3.3). TCO-cetuximab (3 mg/mL) was then mixed with 1, 2, 5, or 10 equivalents of Tz-DNA barcode and incubated at room temperature for 1 h. Antibody-barcode conjugation was validated by SDS-PAGE without any purification (Figure S2). Using substoichiometric amounts of DNA (1 or 2 equivalents) such that the TCO-sites on the antibody are in excess ensures complete consumption of the Tz-DNA and eliminates the need for further purification.

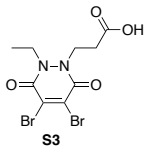
## SYNTHESIS



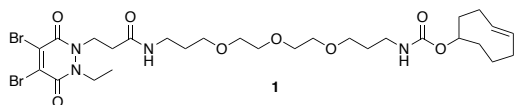
**Scheme S1.** Synthesis of rebridging agent PD-TCO **1**

**S1** was synthesized as previously published.<sup>6</sup> Bromoethane (319  $\mu$ L, 4.31 mmol) was added to a solution of di-tert-butyl hydrazodiformate (5.0 g, 21.5 mmol, 5 Eq) and cesium carbonate (2.81 g, 8.61 mmol, 2 Eq) in 30 mL DMF and left to stir at room temperature overnight. The reaction mixture was diluted with 50 mL EtOAc and extracted with deionized (DI) water (2 x 25 mL) and brine (2 x 25 mL). The organic phase was concentrated in vacuo and cold hexane was added to precipitate excess di-tert-butyl hydrazodiformate as a white solid. Following filtration of the white solid, the filtrate was concentrated in vacuo and purified by flash column chromatography (5-25% EtOAc:Hexanes) to give **S1** (485 mg, 43%) as a white solid. NMR characterization matched reported values.<sup>6</sup> <sup>1</sup>H NMR (CDCl<sub>3</sub>, 400 MHz, rotamers present)  $\delta$  6.13 (br. d, 1H), 3.53 – 3.44 (m, 2H), 1.50 – 1.44 (m, 18H), 1.14 (t,  $J$  = 7.2 Hz, 3H). <sup>13</sup>C NMR (CDCl<sub>3</sub>, 100 MHz, rotamers present)  $\delta$  155.3, 81.1, 81.0, 45.7, 44.2, 28.3, 28.3, 12.8.

To a solution of **S1** (437 mg, 1.68 mmol) in 2.5 mL t-BuOH was added 83  $\mu$ L 10% NaOH and left to stir at room temperature for 10 minutes. Tert-butyl acrylate (983  $\mu$ L, 6.71 mmol, 4 Eq) was added to the reaction and the mixture was heated at 60 °C overnight. After this, the reaction mixture was concentrated in vacuo and dissolved in EtOAc (25 mL) and extracted with DI water (3 x 10 mL). The organic phase was dried over MgSO<sub>4</sub> and concentrated in vacuo followed by purification by flash column chromatography (5-25% EtOAc:Hexanes) to give **S2** (377 mg, 58%) as a colorless oil. <sup>1</sup>H NMR (CDCl<sub>3</sub>, 400 MHz, rotamers present)  $\delta$  3.73 – 3.58 (m, 2H), 3.53 – 3.34 (m, 2H), 2.58 (q,  $J$  = 7.6, 7.0 Hz, 2H), 1.50 – 1.39 (m, 27H), 1.15 (t,  $J$  = 7.2 Hz, 3H). <sup>13</sup>C NMR (CDCl<sub>3</sub>, 100 MHz, rotamers present)  $\delta$  171.1, 155.0, 154.8, 81.1, 81.0, 80.8, 46.0, 44.3, 34.1, 28.4, 28.3, 28.2, 12.9. ESI <sup>M+Na+</sup> calculated 411.25 for C<sub>19</sub>H<sub>36</sub>N<sub>2</sub>O<sub>6</sub>Na<sup>+</sup>; observed 411.45.



Dibromomaleic acid (333 mg, 1.22 mmol, 1.5 Eq) was dissolved in 8 mL acetic acid and refluxed at 118 °C for 30 minutes. **S2** (315 mg, 0.81 mmol) was added to the solution and the reaction was heated under reflux for 4 more hours. The reaction mixture was concentrated in vacuo using toluene as an azeotrope (3 x 10 mL) then purified by flash column chromatography (50-100% EtOAc:Hexanes (+1% AcOH)) to give **S3** (177 mg, 59%) as a yellow solid. <sup>1</sup>H NMR (DMSO-d<sub>6</sub>, 400 MHz) δ 12.61 (br. s, 1H), 4.23 (t, *J* = 7.0 Hz, 2H), 4.08 (q, *J* = 6.3 Hz, 2H), 2.58 (t, *J* = 7.0 Hz, 2H), 1.14 (t, *J* = 6.7 Hz, 3H). <sup>13</sup>C NMR (DMSO-d<sub>6</sub>, 100 MHz) δ 171.9, 153.1, 152.7, 135.6, 135.3, 42.8, 42.3, 31.6, 12.7. ESI <sup>M+H</sup> calculated 366.89, 368.89, 370.89 (1:2:1) for C<sub>9</sub>H<sub>9</sub>Br<sub>2</sub>N<sub>2</sub>O<sub>4</sub><sup>-</sup>; observed 367.06, 369.06, 371.10 (1:2:1).



HATU (32.2 mg, 84.7 μmol, 1.5 Eq), DIPEA (14.8 μL, 11.0 mg, 84.7 μmol, 1.5 Eq), and TCO-PEG<sub>3</sub>-Amine (Click Chemistry Tools, #1188, 21.0 mg, 56.5 μmol, 1 Eq) was added to a solution of **S3** (20.9 mg, 56.5 μmol) in DMSO and left stirring for 10 minutes. LC-MS verified consumption of the starting materials. The reaction mixture was loaded directly onto a Biotage Snap Bio C18 column and purified by reverse phase flash chromatography (5-100% MeOH:Water) to give **1** (17.8 mg, 44%) as a yellow solid. <sup>1</sup>H NMR (DMSO-d<sub>6</sub>, 400 MHz) δ 7.99 (t, *J* = 5.2 Hz, 1H), 6.91 (t, *J* = 5.0 Hz, 1H), 5.57 (ddd, *J* = 14.7, 10.1, 4.0 Hz, 1H), 5.48 – 5.37 (m, 1H), 4.27 – 4.15 (m, 3H), 4.08 (q, *J* = 6.9 Hz, 2H), 3.55 – 3.42 (m, 8H), 3.39 – 3.31 (m, 4H), 3.00 (dq, *J* = 19.9, 6.3 Hz, 4H), 2.39 (t, *J* = 6.7 Hz, 2H), 2.30 – 2.16 (m, 3H), 1.95 – 1.78 (m, 4H), 1.66 – 1.46 (m, 7H), 1.13 (t, *J* = 6.9 Hz, 3H). <sup>13</sup>C NMR (DMSO-d<sub>6</sub>, 100 MHz) δ 169.0, 155.8, 153.1, 152.7, 135.6, 135.3, 134.9, 132.6, 78.9, 69.8, 69.6, 68.0, 67.9, 43.6, 42.0, 40.7, 38.3, 37.5, 35.8, 33.8, 33.3, 32.2, 30.6, 29.7, 29.2, 12.6. ESI <sup>M+H</sup> expected 723.16, 725.16, 727.16 (1:2:1) for C<sub>28</sub>H<sub>45</sub>Br<sub>2</sub>N<sub>4</sub>O<sub>8</sub><sup>+</sup>; observed 723.47, 725.51, 727.43 (1:2:1).

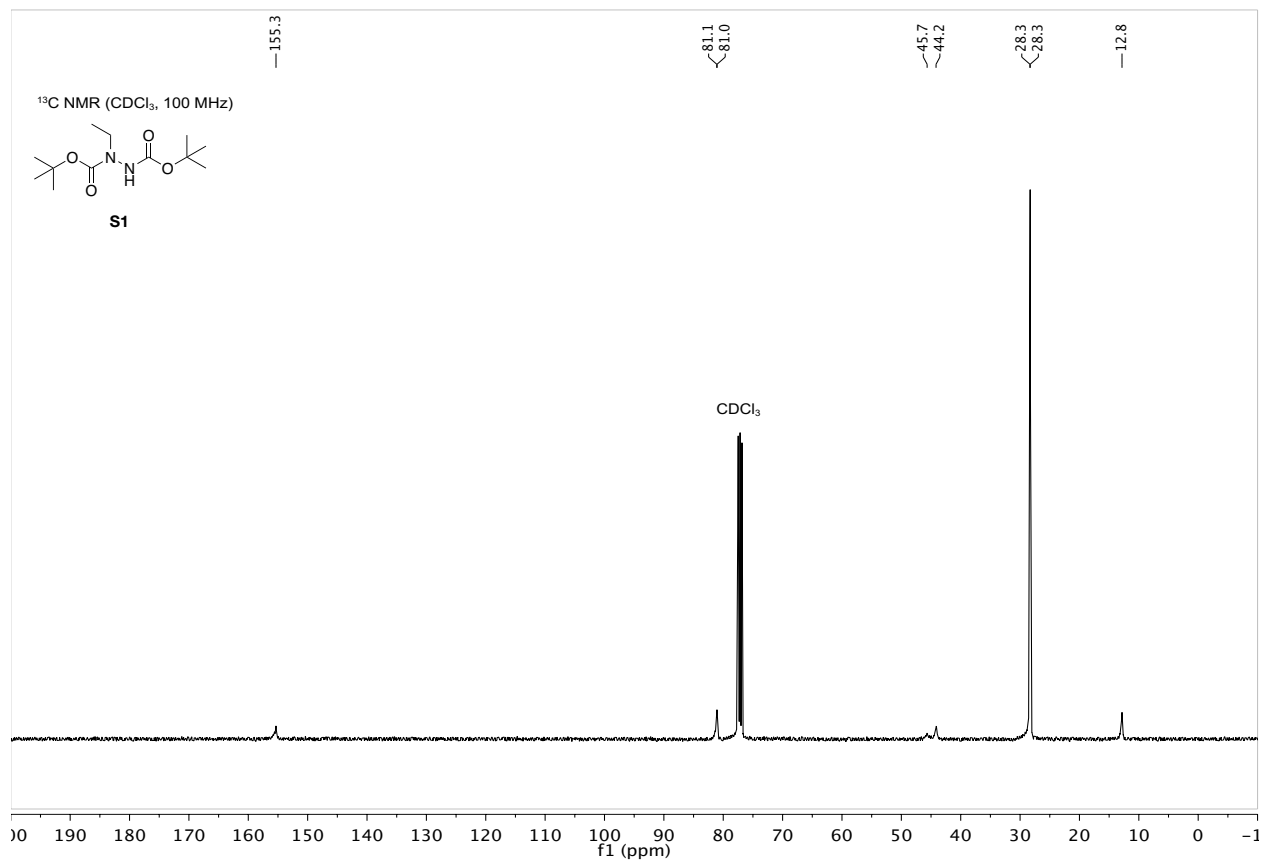
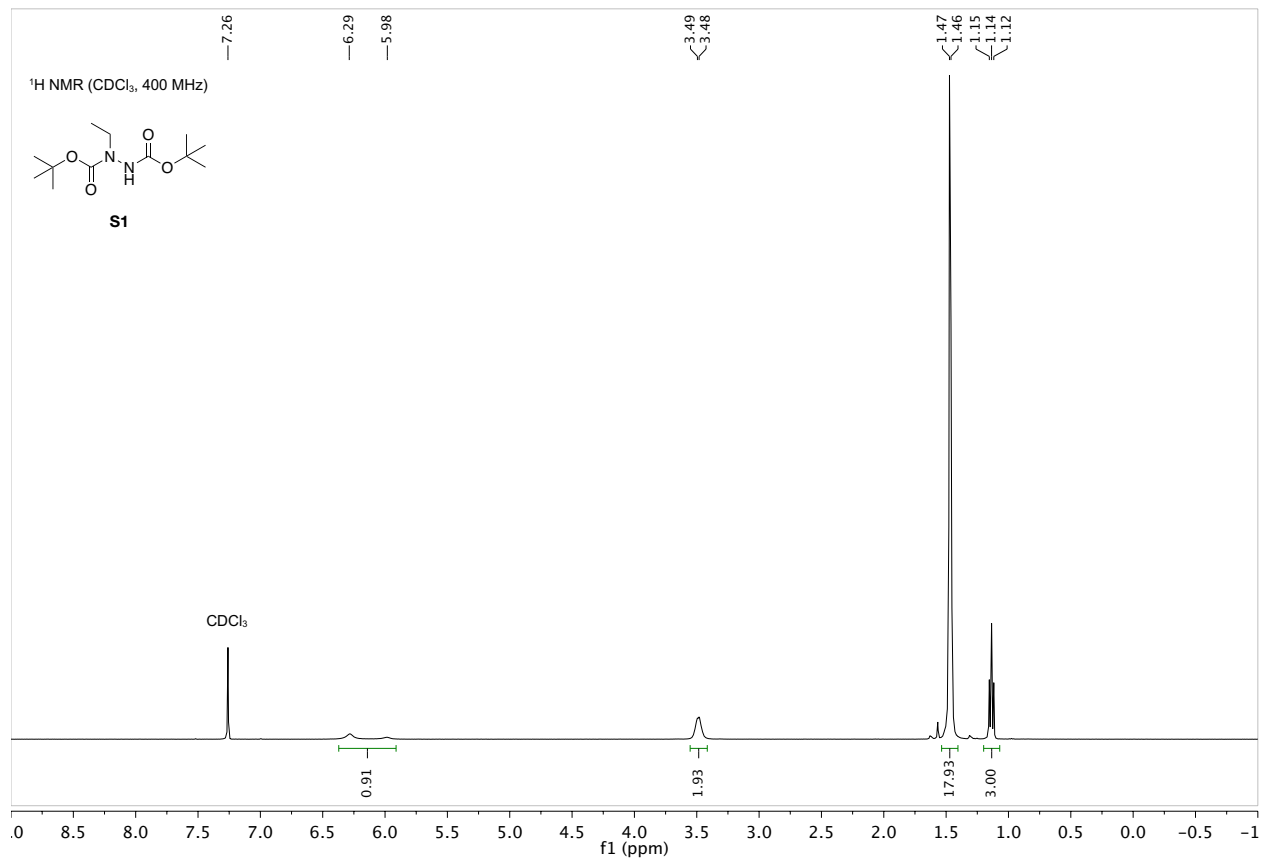


**Figure S10.** <sup>1</sup>H and <sup>13</sup>C NMR spectra of **S1**.

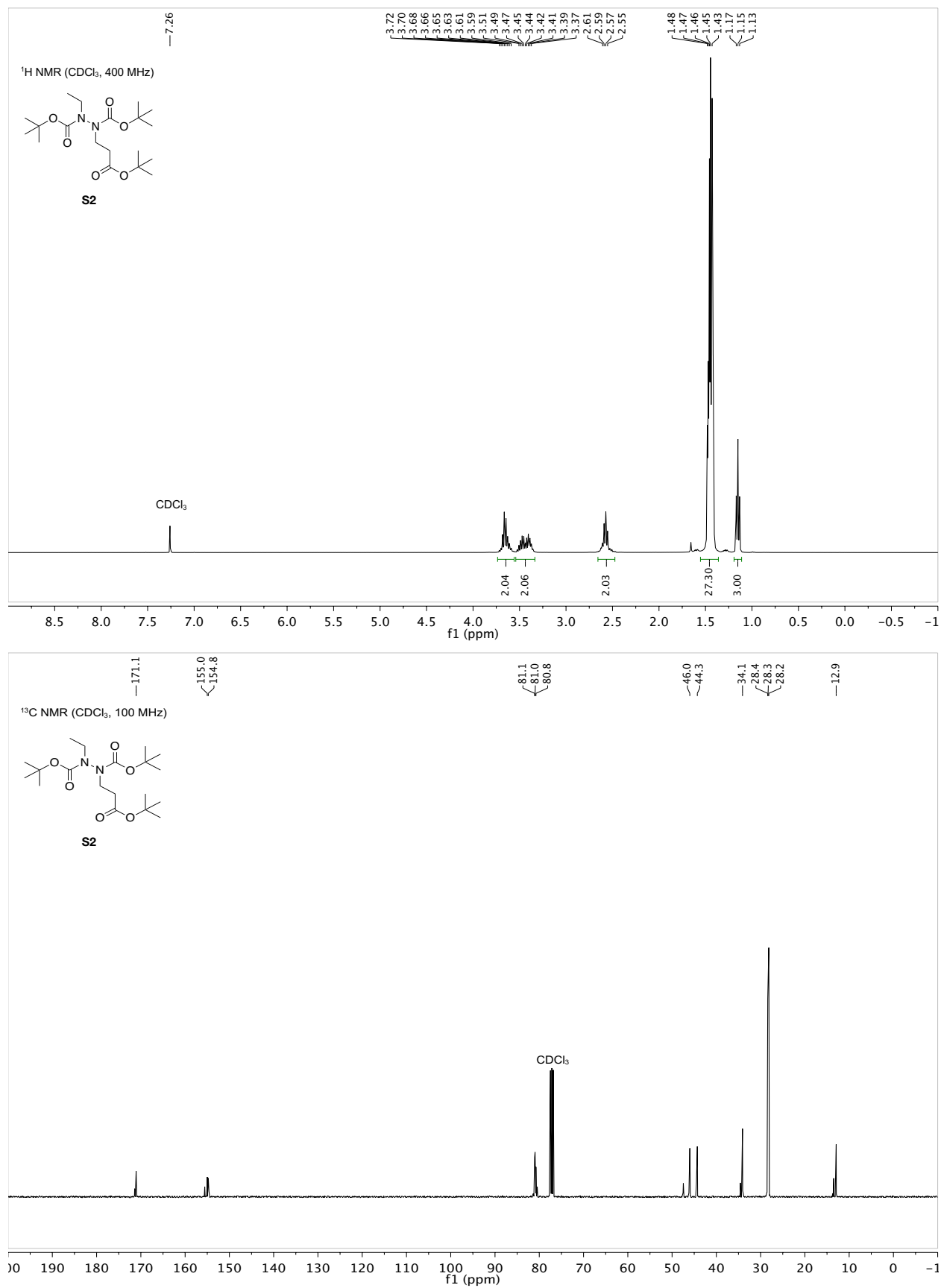


**Figure S11.** <sup>1</sup>H and <sup>13</sup>C NMR spectra of **S2**.



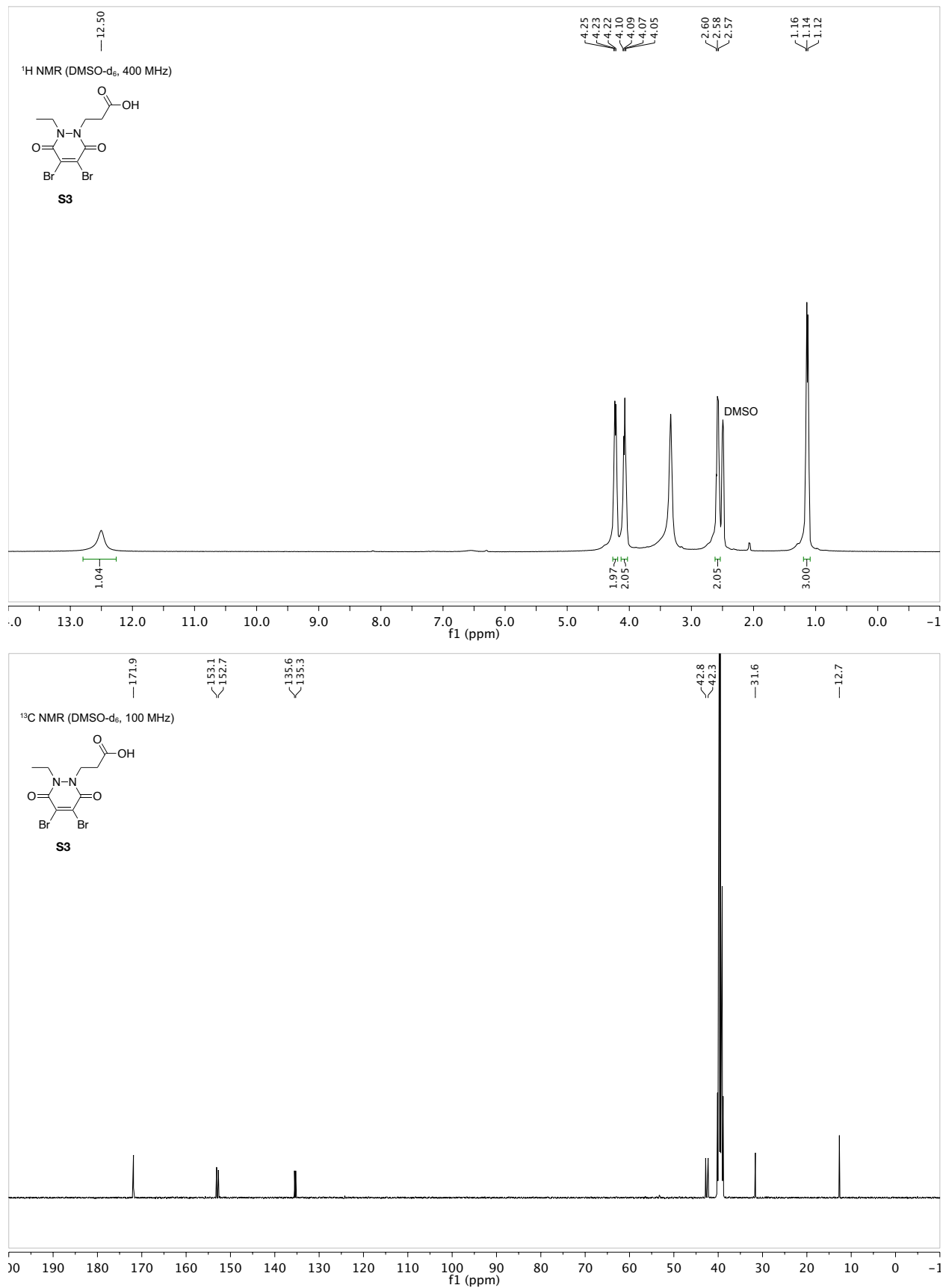


**Figure S12.** <sup>1</sup>H and <sup>13</sup>C NMR spectra of **S3**.

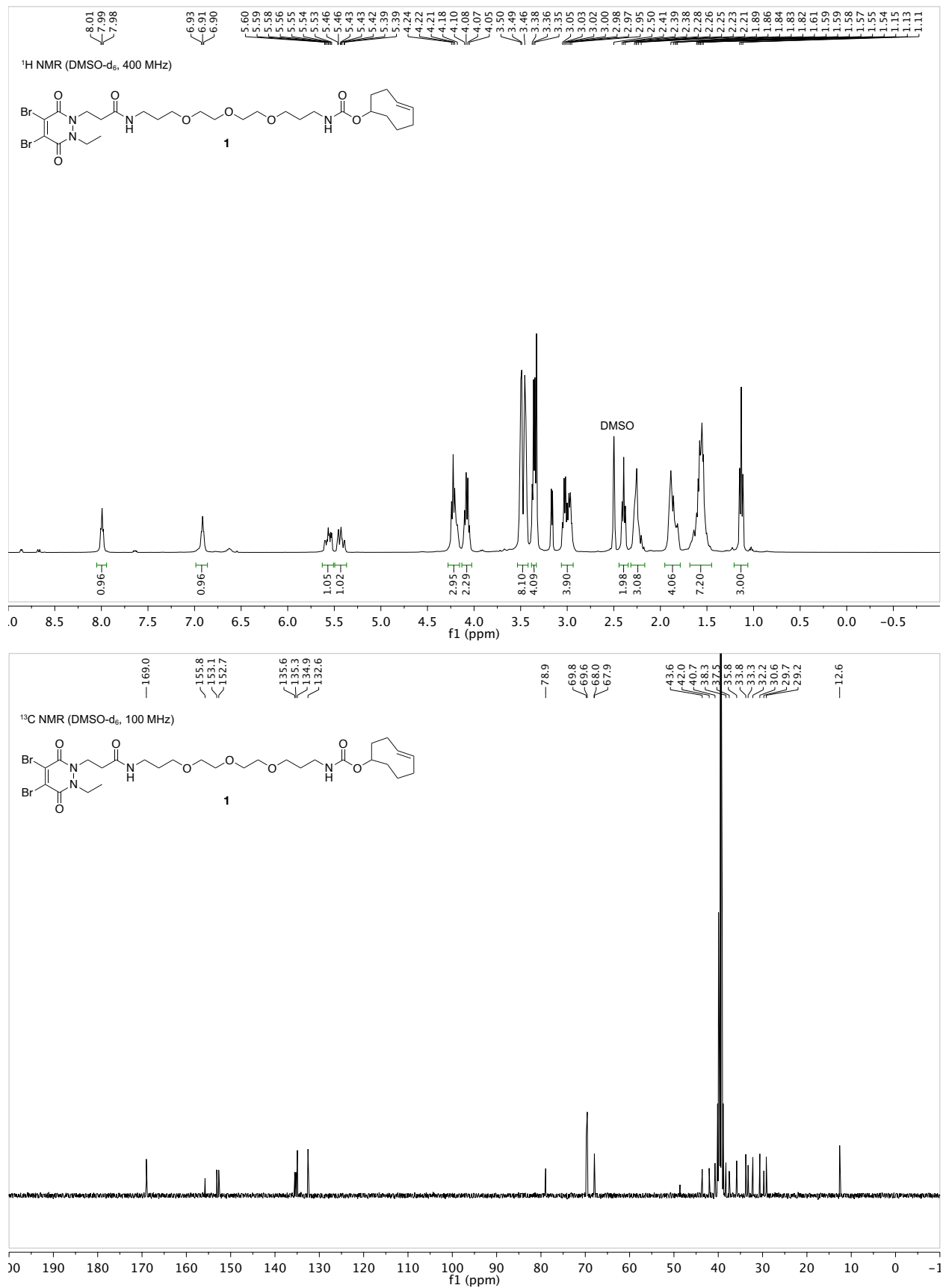


**Figure S13.** <sup>1</sup>H and <sup>13</sup>C NMR spectra of **1**.

## REFERENCES

- (1) Burton, D. R. (1985) Immunoglobulin G: functional sites. *Mol. Immunol.* 22, 161-206.
- (2) Clark, M. R. (1997) Antibody Engineering. *Chem. Immunol.* 65, 88-110.
- (3) Dangl, J. L., Wensel, T. G., Morrison, S. L., Stryer, L., Herzenberg, L. A. and Oi, V. T. (1988) Segmental flexibility and complement fixation of genetically engineered chimeric human, rabbit and mouse antibodies. *The EMBO Journal* 7, 1989-1994.
- (4) Liu, H. and May, K. (2012) Disulfide bond structures of IgG molecules: structural variations, chemical modifications and possible impacts to stability and biological function. *MABs* 4, 17-23.
- (5) Fuss, I. J., Kanof, M. E., Smith, P. D. and Zola, H. (2009) Isolation of whole mononuclear cells from peripheral blood and cord blood. *Curr. Protoc. Immunol.* 85, 7.1.1-7.1. 8.
- (6) Lee, M. T. W., Maruani, A., Baker, J. R., Caddick, S. and Chudasama, V. (2016) Next-generation disulfide stapling: reduction and functional re-bridging all in one. *Chem. Sci.* 7, 799-802.